

OLFACTORY SENSING / TRANSDUCTION

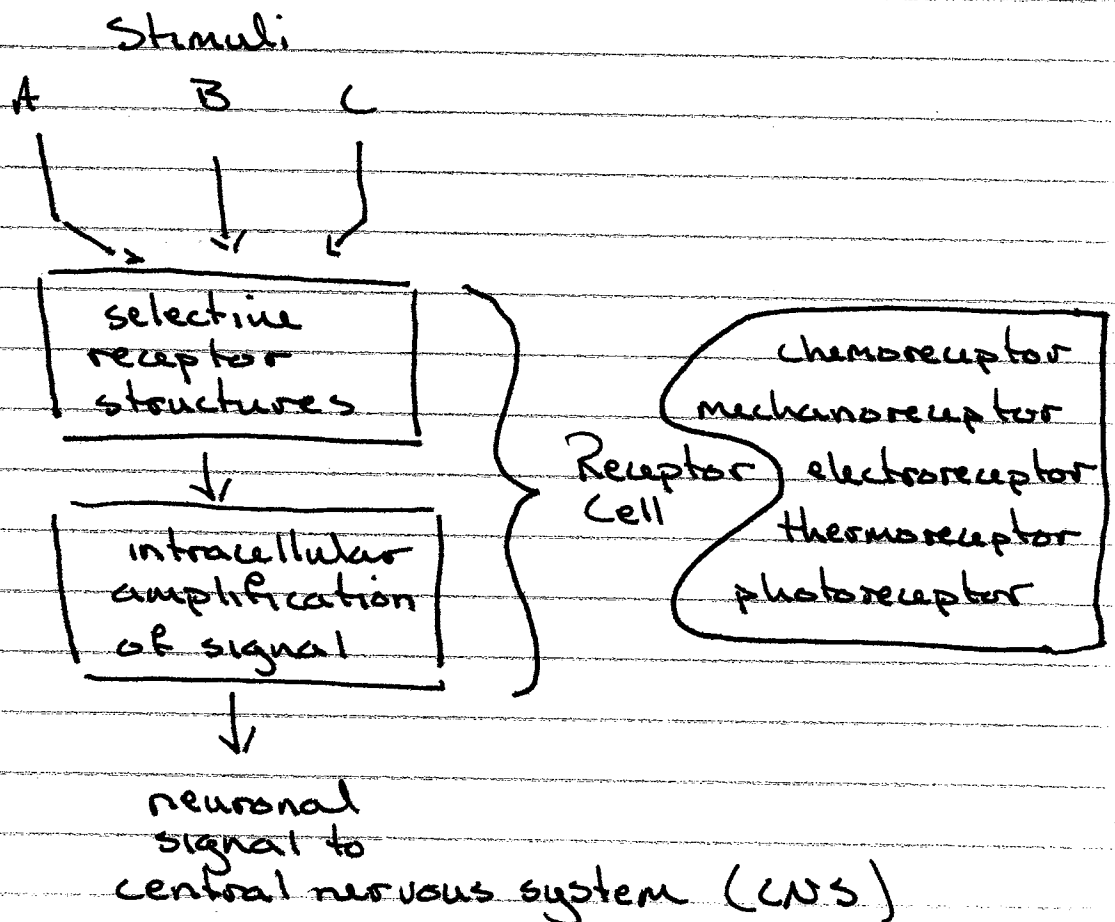
Overview: "Sensing the Environment"

source: Eckert. Animal Physiology.

organisms, all of them, must be 'aware' of the external (and internal) environment.

The issues associated with environmental sensing are probably most acute in sessile organisms, plants and fungi. But, even animals depend on receiving environmental information, and interpreting, and responding to it.

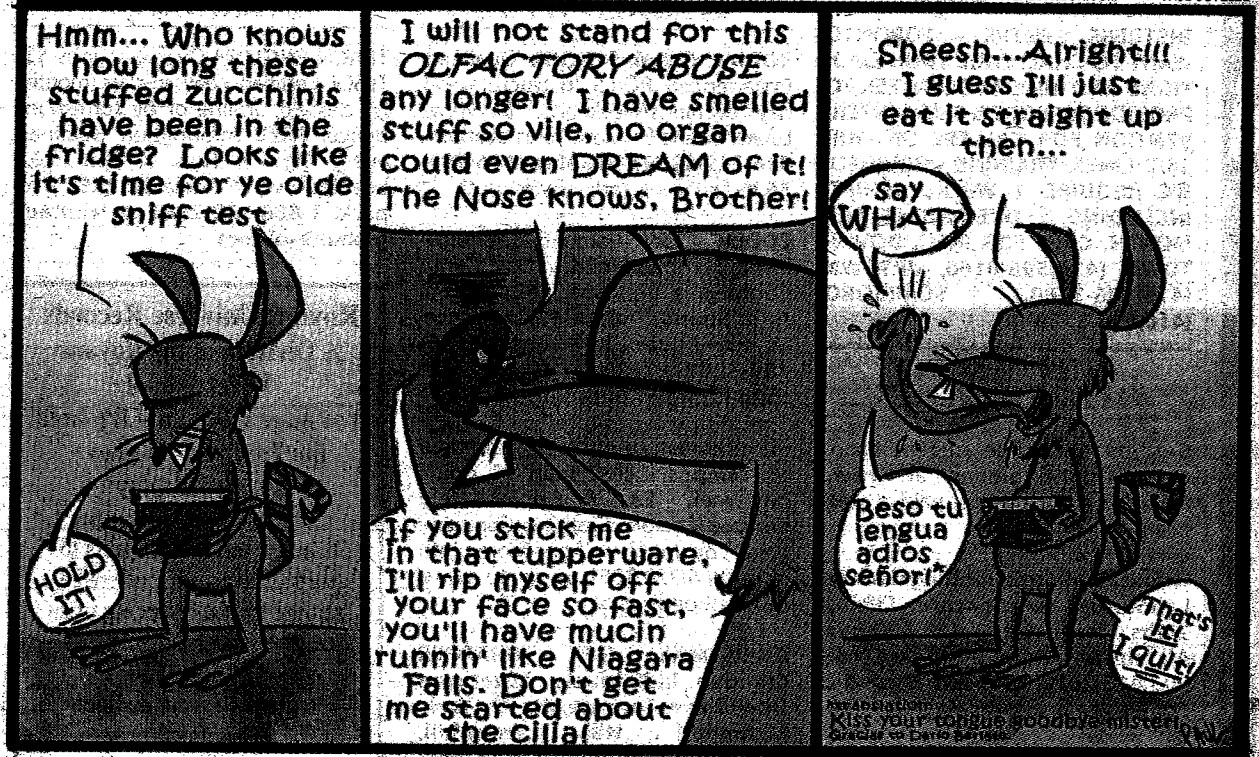
In animals, the general schema:



The Importance of Olfaction is Exemplified by The Fertile Imagination of Paul Covello

Evil Steve

EVILSTEVE.VEALONABUN.COM PAUL COVELLO



Excalibur, York University, Fall, 2004

PHYSICS OF CHEMORECEPTION

HOWARD C. BERG AND EDWARD M. PURCELL, *Department of Molecular, Cellular, and Developmental Biology, University of Colorado, Boulder, Colorado 80309 and the Department of Physics, Harvard University, Cambridge, Massachusetts 02138 U.S.A.*

ABSTRACT Statistical fluctuations limit the precision with which a microorganism can, in a given time T , determine the concentration of a chemoattractant in the surrounding medium. The best a cell can do is to monitor continually the state of occupation of receptors distributed over its surface. For nearly optimum performance [only a small fraction of the surface need be specifically adsorbing.] The probability that a molecule that has collided with the cell will find a receptor is $Ns/(Ns + \pi a)$, if N receptors, each with a binding site of radius s , are evenly distributed over a cell of radius a . There is ample room for many independent systems of specific receptors. The adsorption rate for molecules of moderate size cannot be significantly enhanced by motion of the cell or by stirring of the medium by the cell. The least fractional error attainable in the determination of a concentration \bar{c} is approximately $(T\bar{c}aD)^{-1/2}$, where D is the diffusion constant of the attractant. The number of specific receptors needed to attain such precision is about a/s . Data on bacteriophage adsorption, bacterial chemotaxis, and chemotaxis in a cellular slime mold are evaluated. The chemotactic sensitivity of *Escherichia coli* approaches that of the cell of optimum design.

BIOPHYSICAL JOURNAL VOLUME 20 1977

* only a small fraction of the surface needs to be specifically absorbing.

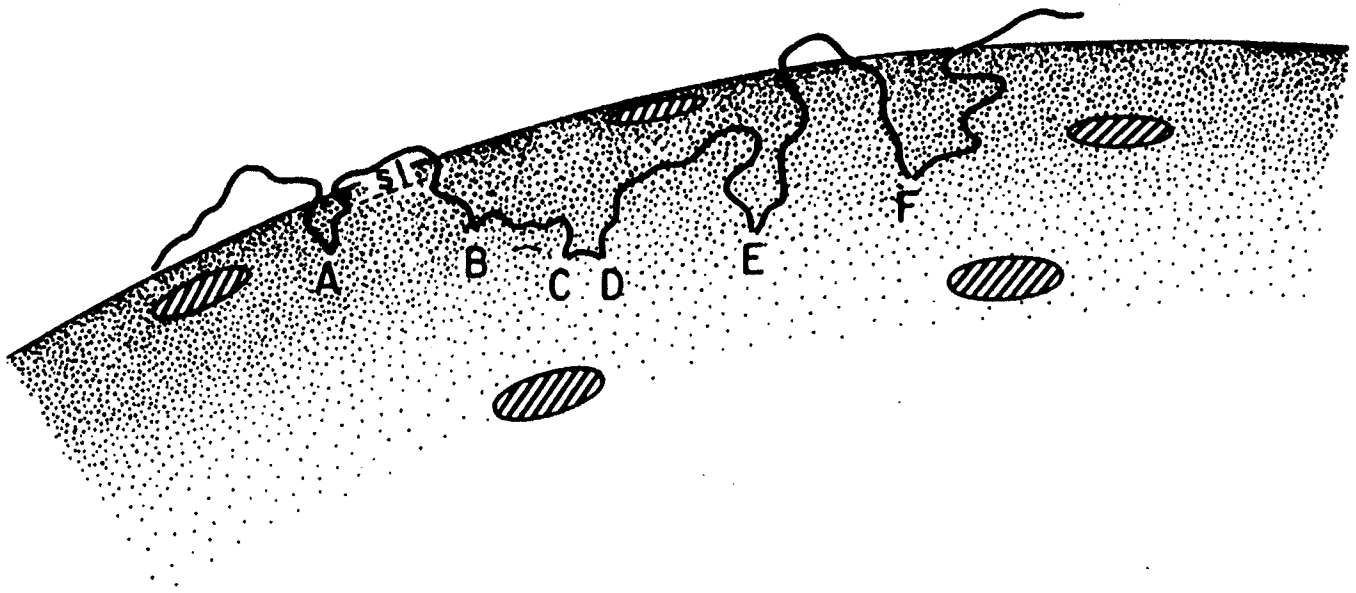


FIGURE 1 The path of a diffusing molecule that has touched the surface of a cell of radius a at a sequence of points A, B, \dots, F . The receptor patches, shown shaded, are of radius s . A and B constitute independent tries at hitting a patch, but C and D do not. Note between A and B the excursion of distance s perpendicular to the surface of the sphere.

In a random walk, the particle will tend to reside near the surface.

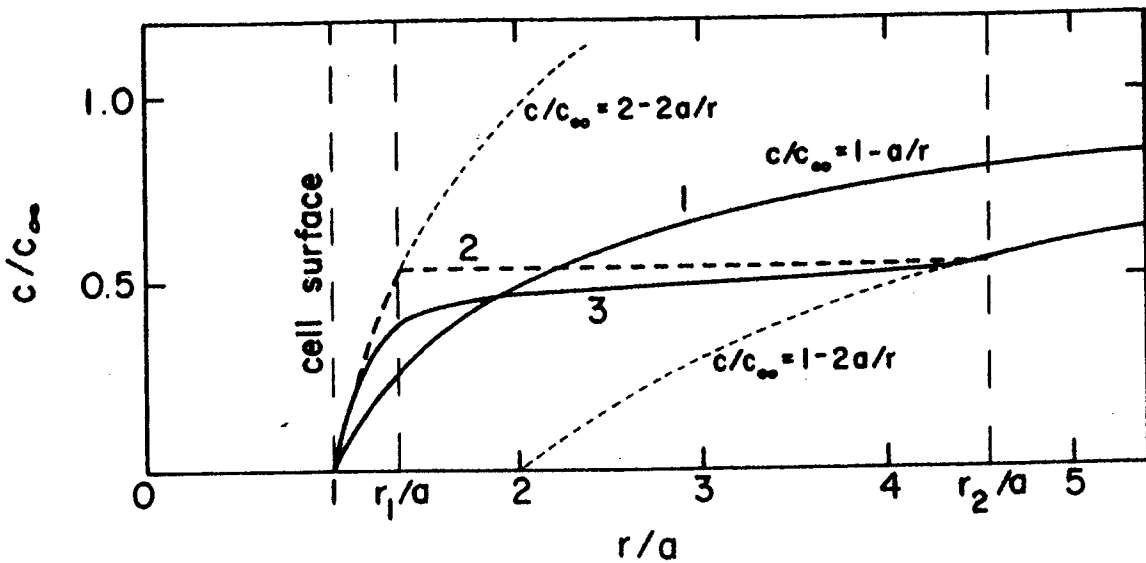
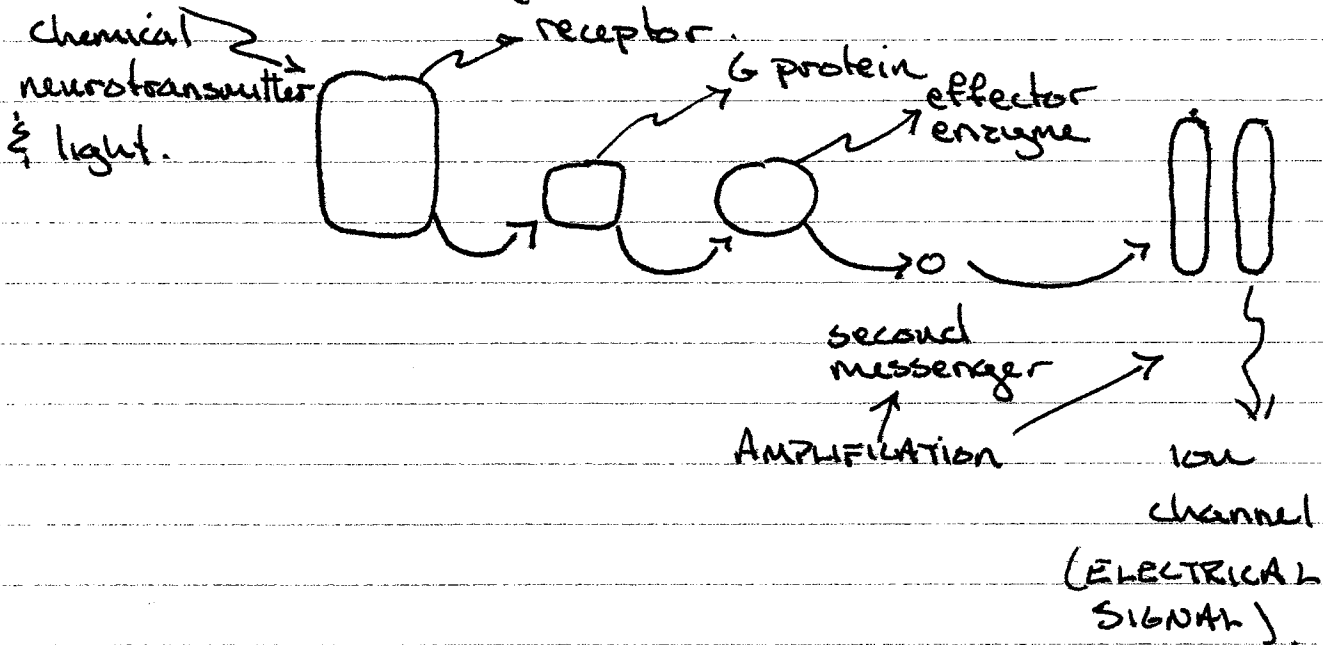


FIGURE 2 Relative concentration in the vicinity of a spherical absorber, for three cases: (1) No stirring; the current absorbed is $J_0 = 4\pi a D c_\infty$. (2) Volume between r_1 and r_2 stirred infinitely rapidly, fluid stationary elsewhere; current absorbed is $2J_0$. (3) Finite stirring speed; region inside r_1 still dominated by diffusion; current absorbed is $2J_0$.

At the level of the cell receptor cell:



In olfaction, insects are a 'perfect' model organism:

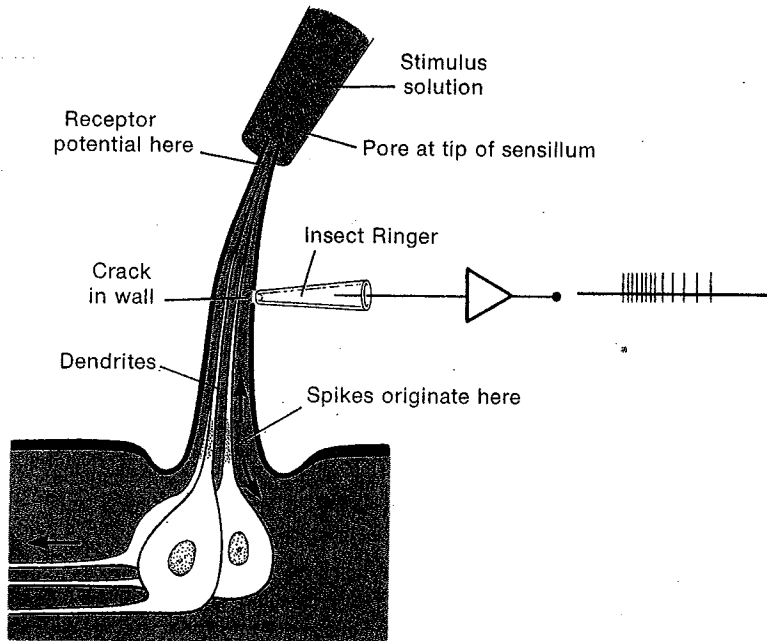


Figure 7-19 The response of a housefly's contact chemoreceptors can be recorded extracellularly. The dendrites of several neurons share a single sensillum. The dendrite of each individual neuron within the sensillum is sensitive to a particular class of substances (e.g., sugars, cations, anions, or water). Stimuli are presented through a cannula slipped over the tip of the sensillum, and electrical responses (in red at right) are recorded through a crack made in the cuticle covering the sensillum.

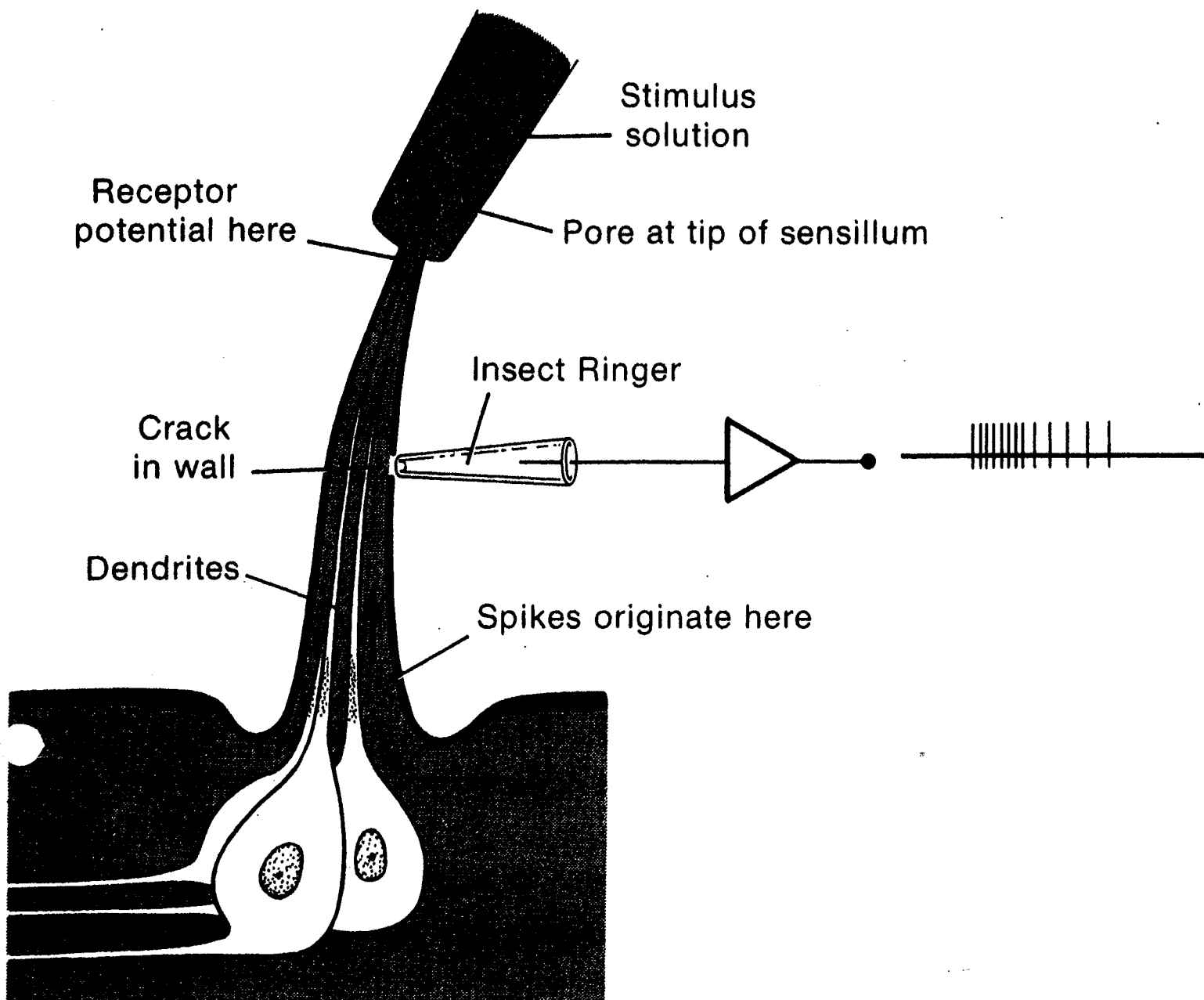


Figure 7-19 The response of a housefly's contact chemoreceptors can be recorded extracellularly. The dendrites of several neurons share a single sensillum. The dendrite of each individual neuron within the sensillum is sensitive to a particular class of substances (e.g., sugars, cations, anions, or water). Stimuli are presented through a cannula slipped over the tip of the sensillum, and electrical responses (in red at right) are recorded through a crack made in the cuticle covering the sensillum.

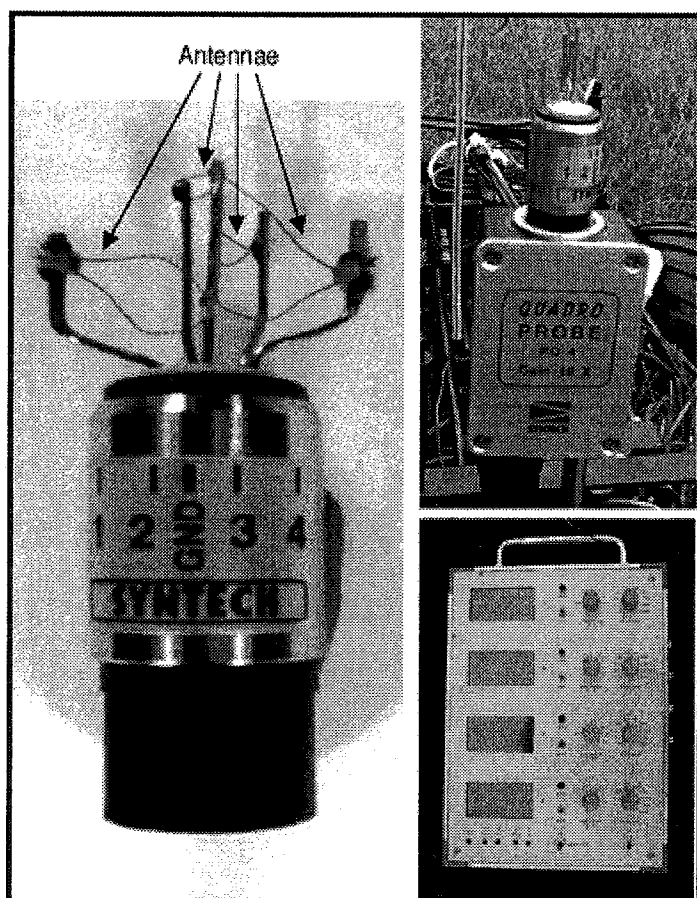
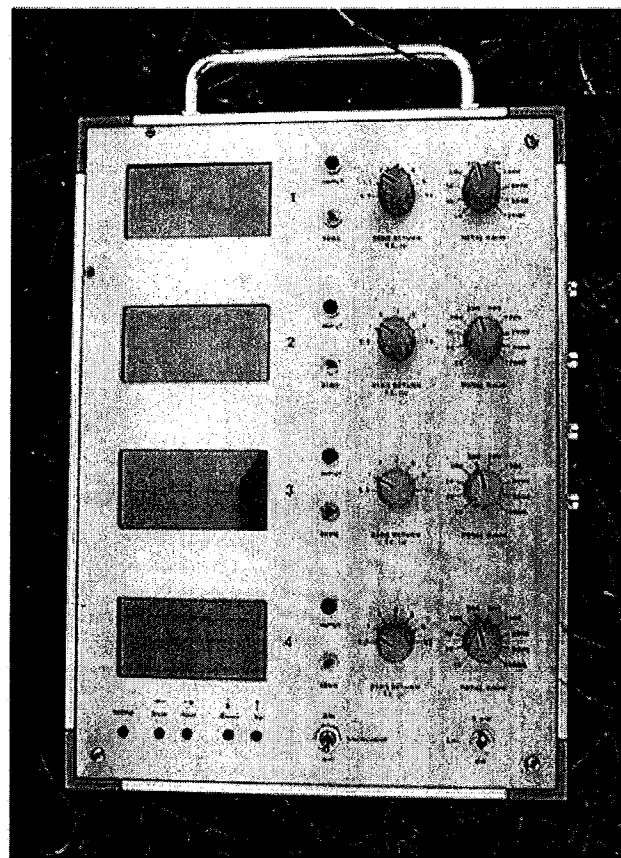


Figure 1 A portable Quadro-probe EAG recording system, enabling simultaneous, real-time EAG recordings from four different insect antennae on site. Electroantennogram signals from the four different antennae mounted on the Quadro-probe stage (left) are conditioned and amplified with a headstage pre-amplifier (top right) and further amplified and monitored with a main amplifier (bottom right).

Antennae



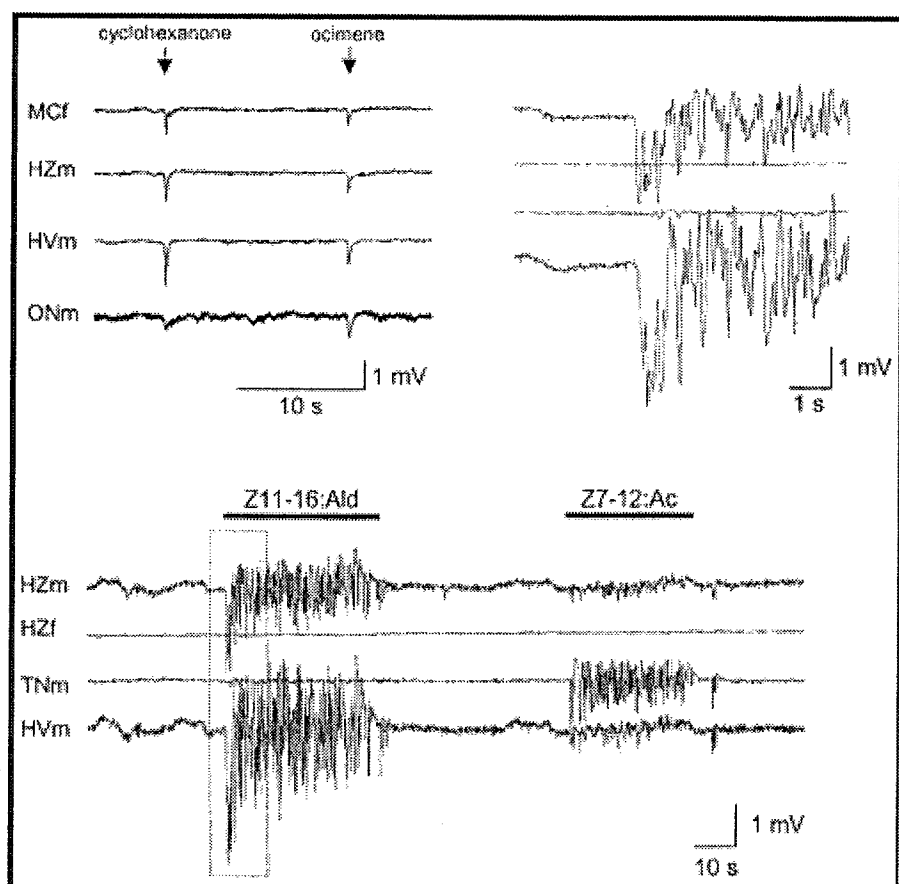
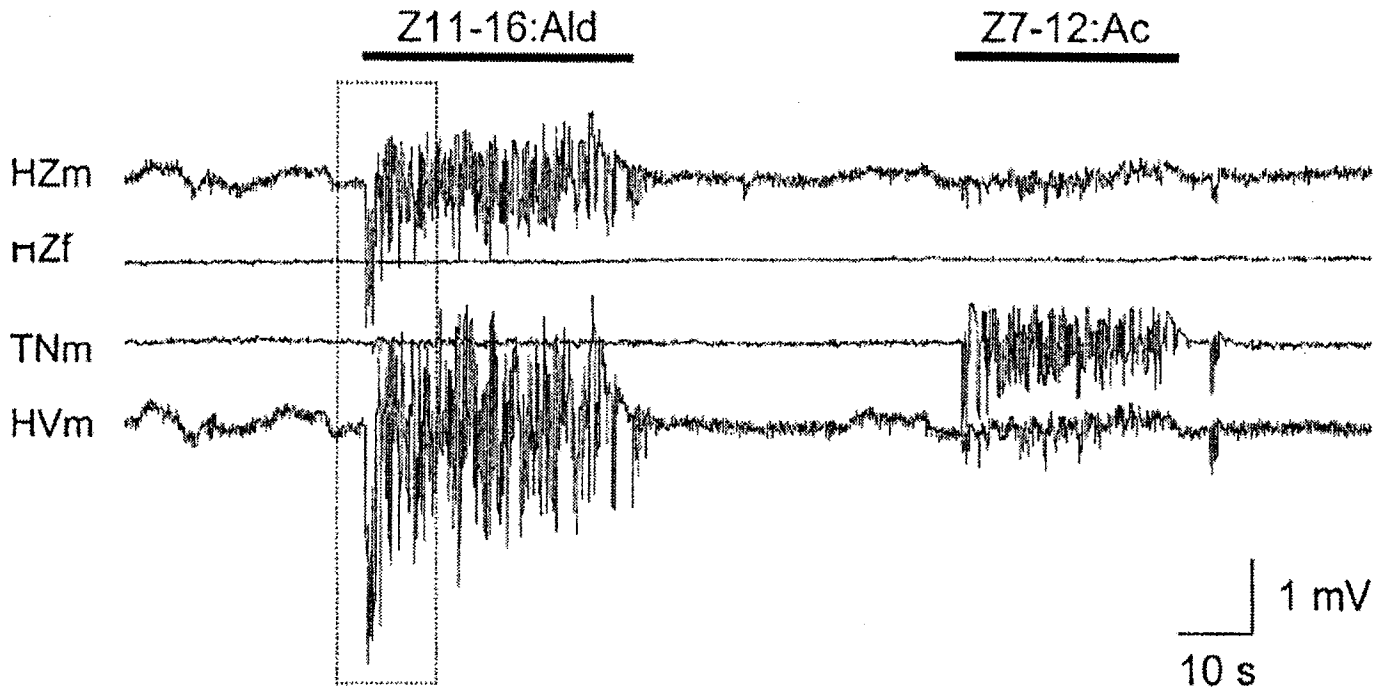
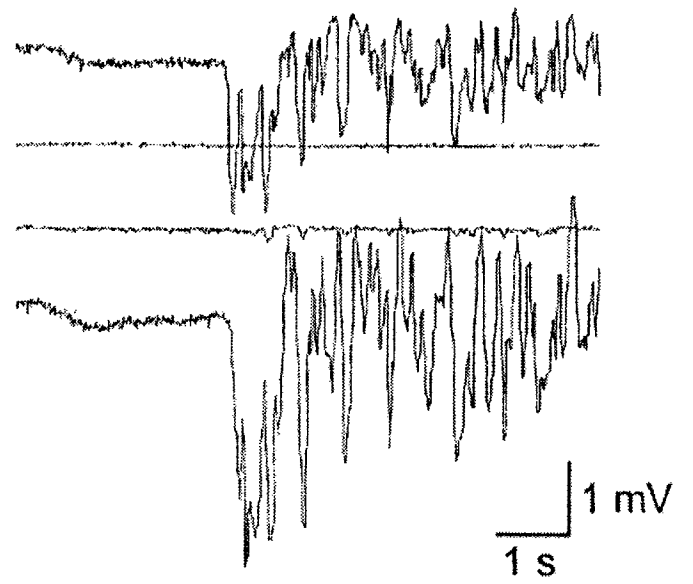
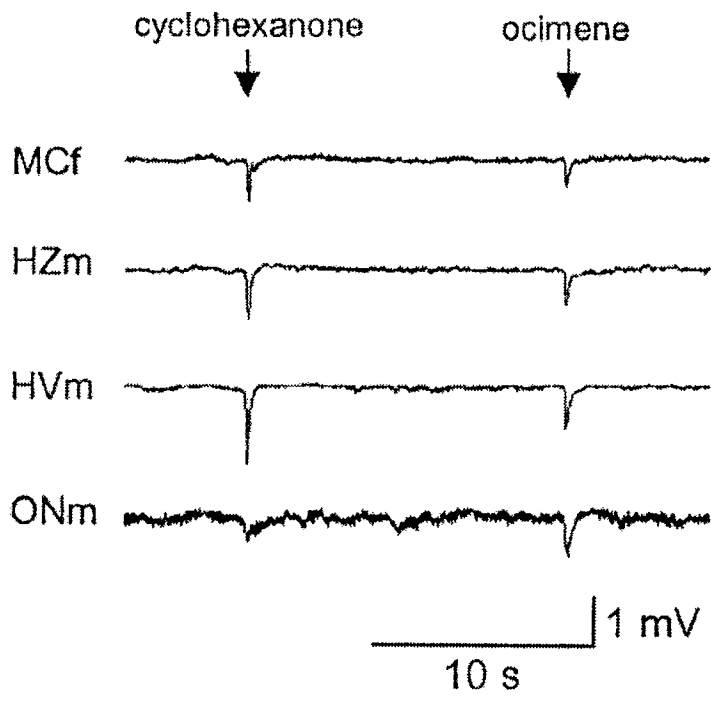


Figure 8 Simultaneously recorded EAG responses elicited by four different antennae mounted on a Quadro-probe in a wind tunnel. Top left: EAG responses to single puffs of two different stimuli. Bottom: EAG responses to two separate continuous odor plumes. Top right shows the details of the responses in the dotted box. MCF, female *M. croceipes*; HZm, male *H. zea*; HVm, male *H. virescens*; ONm, male *O. nubilalis*; HZf, female *H. zea*; TNm, male *T. ni*.



International Conference on Intelligent Robots and Systems-Volume 2
August 05 - 09, 1995, Pittsburgh, Pennsylvania, USA


p. 2530 **Steering control of a mobile robot using insect antennae**

Y. Kuwana, I. Shimoyama, H. Miura, Dept. of Mechano-Inf., Tokyo Univ.,
Japan

A male silk moth (*Bombyx mori*) pursues a female by following a pheromone, called Bombycol. This action is caused by only a few molecules of pheromone which arrive at the antenna of a male silk moth. The antenna has very sharp sensitivity and specificity. In this paper, the use of a biological sensor is discussed as a new type of sensor, in other words "living sensors". The electrical activity of a silk moth antenna, called the electroantennogram (EAG) was obtained using self-made electrodes and amplifier. Two pheromone sensors were attached to a simple mobile robot to determine the direction of a pheromone trace. From this information, we were able to control the direction of the robot. The robot followed the pheromone trace just like a real male silk moth.

Index Terms- chemioception; zoology; mobile robots; chemical sensors; mobile robot; steering control; insect antennae; *Bombyx mori*; male silk moth; pheromone; Bombycol; biological sensor; living sensors; electrical activity; electroantennogram; EAG

<http://csdl.computer.org/comp/proceedings/iros/1995/7108/02/71082530abs.htm>


IEEE
COMPUTER
SOCIETY
<http://computer.org/>



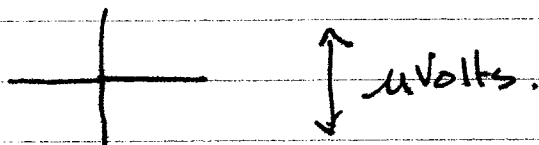
Mosquito Mania / *The New York Times*

OLFACTION: Carbon dioxide sensing in blood-feeding insects, including mosquito.

Method.

A sharpened tungsten wire is inserted into the sensillum[⊕]. A reference electrode is inserted into the eye.

The tungsten electrode measures very small electrical changes in the area surrounding the neuron(s). These are visible as fast voltage transients:



(see example on overhead).

Then, streams of air ± the test compound are blown over the sensillum. With care, it is possible to apply the test compound very rapidly.

⊕ Note that sensilla are found in a variety of places: antenna, mouthparts, legs etc.

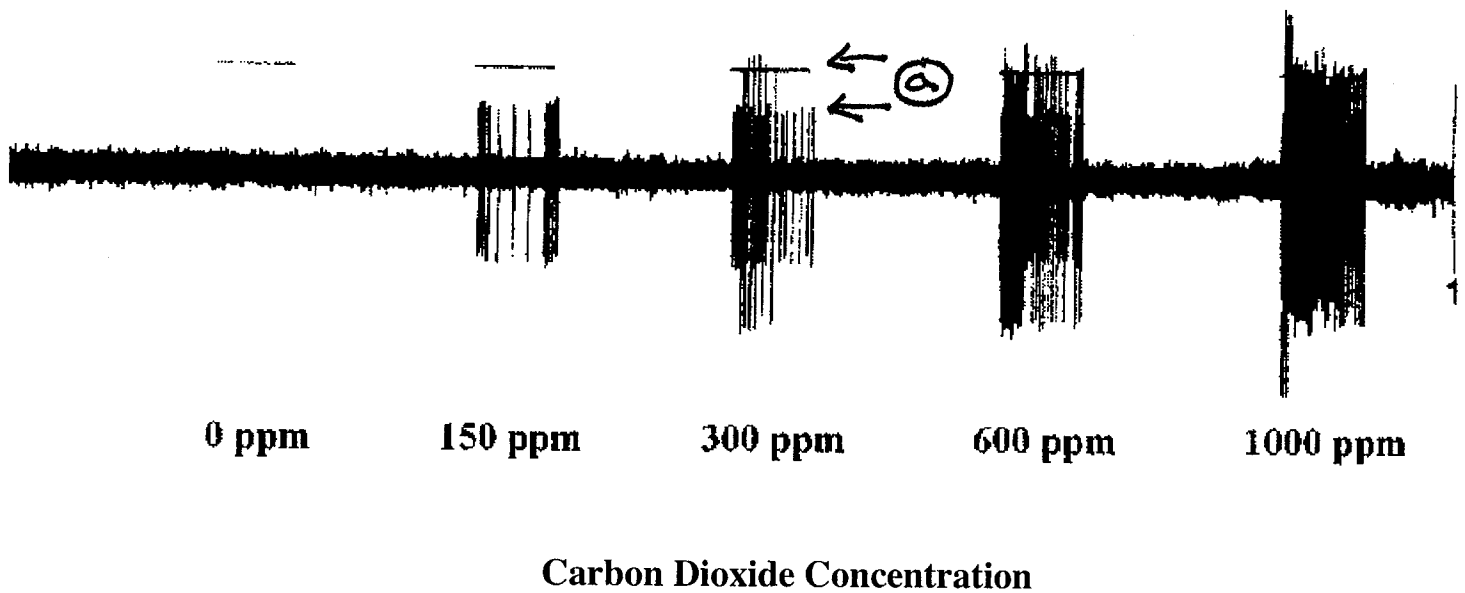


Fig. 2. Electrophysiological recordings from the maxillary palp sensilla of *C. furens* in response to stimulation with different concentrations of carbon dioxide. In this particular example, two amplitude action potentials are present. The neuron producing each set of action potentials responds to increasing concentrations of CO₂. The bars above the trace indicate the timing and duration of the 2-s stimulus pulse (0, 150, 300, 600, 1000 ppm CO₂). Between stimulations the preparation was held in a background environment of 0-ppm CO₂.

Electrophysiological Responses from *Culicoides* (Diptera: Ceratopogonidae) to Stimulation with Carbon Dioxide

ALAN J. GRANT AND DANIEL L. KLINE

American Biophysics Corp., 2240 South County Trail, East Greenwich, RI 02818

J. Med. Entomol. 40(3): 284-293 (2003)

Ⓐ Two action potential 'levels' are observed, implying that two distinct neurons are being sampled by the sharpened tungsten wire. The level of neuronal excitation is measured by the number of electrical transients occurring over some period of time.

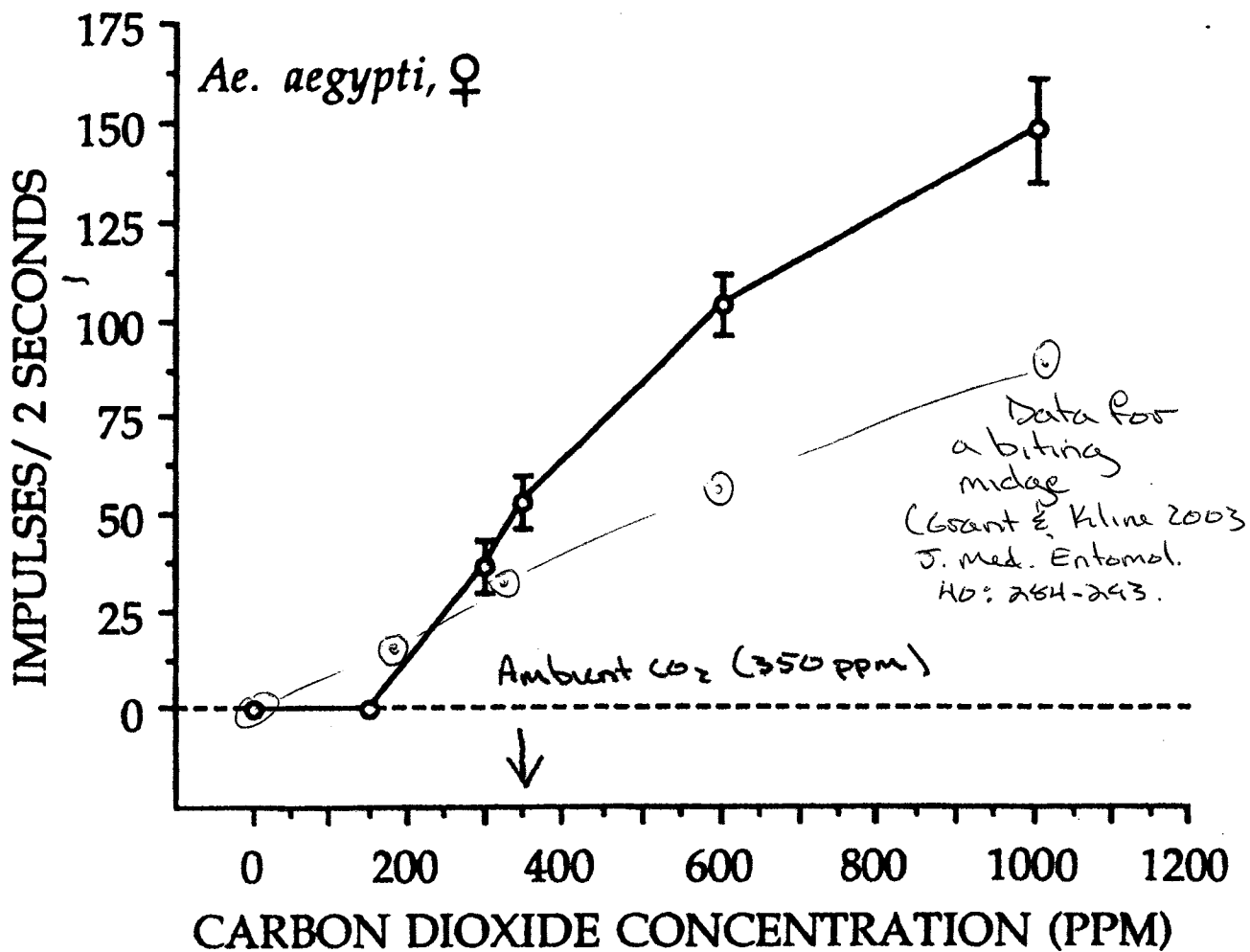


Fig. 2 Average (\pm SEM) number of action potentials during 2 s stimulus pulses of the indicated concentrations of CO₂ from 13 receptor neurons in *s. basiconica* on the maxillary palps of 11 female *Ae. aegypti*. These responses were obtained in a synthetic air background containing 0 ppm CO₂

Electrophysiological Responses of Receptor Neurons in Mosquito Maxillary Palp Sensilla to Carbon Dioxide

A.J. Grant, B.E. Wigton, J.G. Aghajanian, and R.J. O'Connell.
Worcester Foundation for Biomedical Research, Shrewsbury, MA
American Biophysics Corp., Jamestown, RI
J. Comp. Physiol. A (1995) 177: 389-396

Note that ambient CO₂ background is about 350 ppm
It may be possible that the sensitivity at less than ambient CO₂ is due to evolution of the CO₂ receptor when ambient CO₂ was much lower.

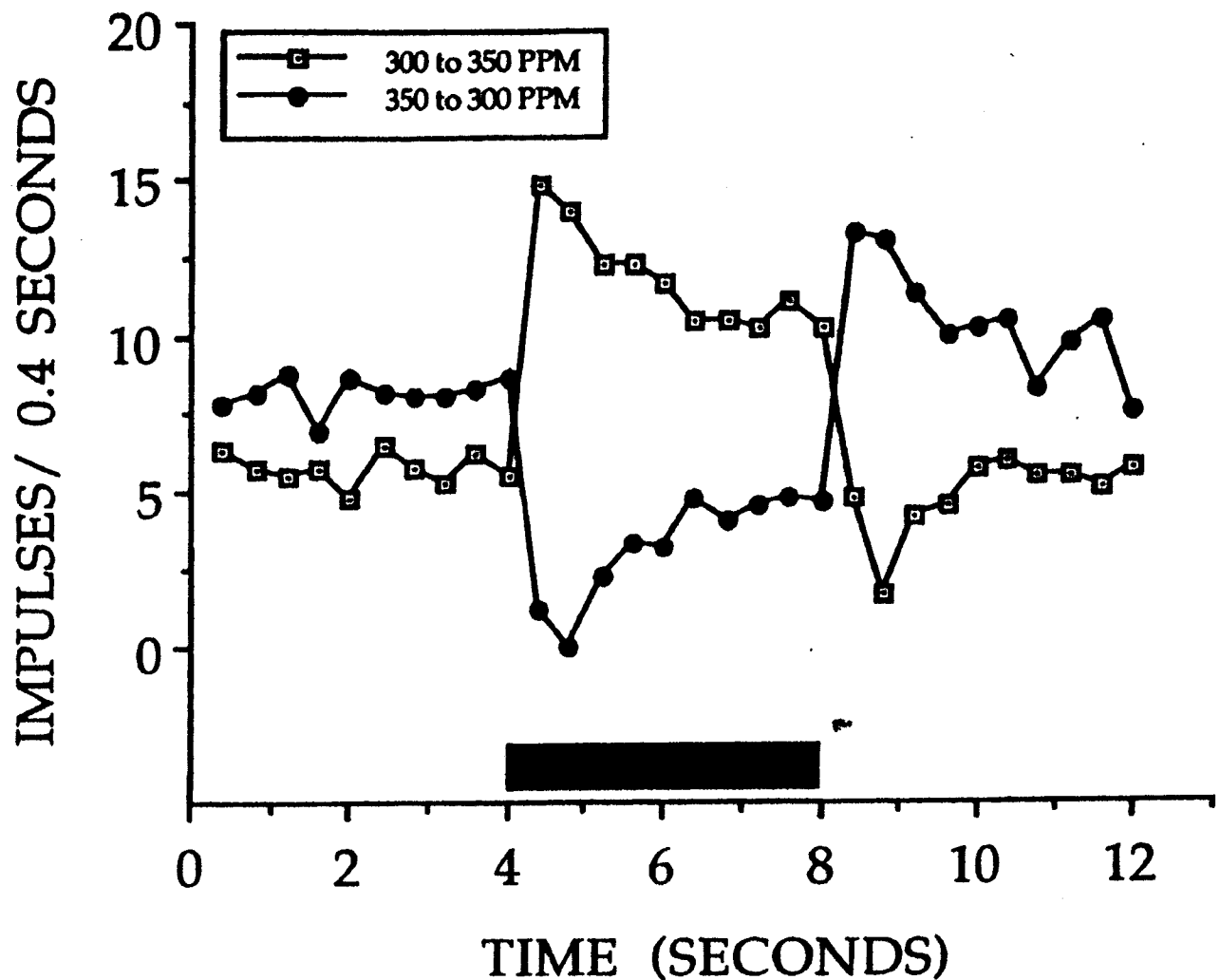


Fig. 3 The temporal pattern of response of a CO₂ receptor neuron, in a *s. basicornicum* on the maxillary palp of a female *Ae. aegypti*. The *open symbols* represent the average response to a 4 s stimulus pulse up to 350 ppm CO₂ from a background concentration of 300 ppm. The *solid symbols* represent the average response to a 4 s stimulus pulse down to 300 ppm from a background level of 350 ppm CO₂. In both cases the number of action potentials were averaged in 400 ms time bins and represent the mean from a single sensillum stimulated 10 times with each pulse protocol. The data acquired during the 4 s purge of the stimulus line just before the onset of the stimulus, is not displayed

The response peaks quickly after the change in CO₂

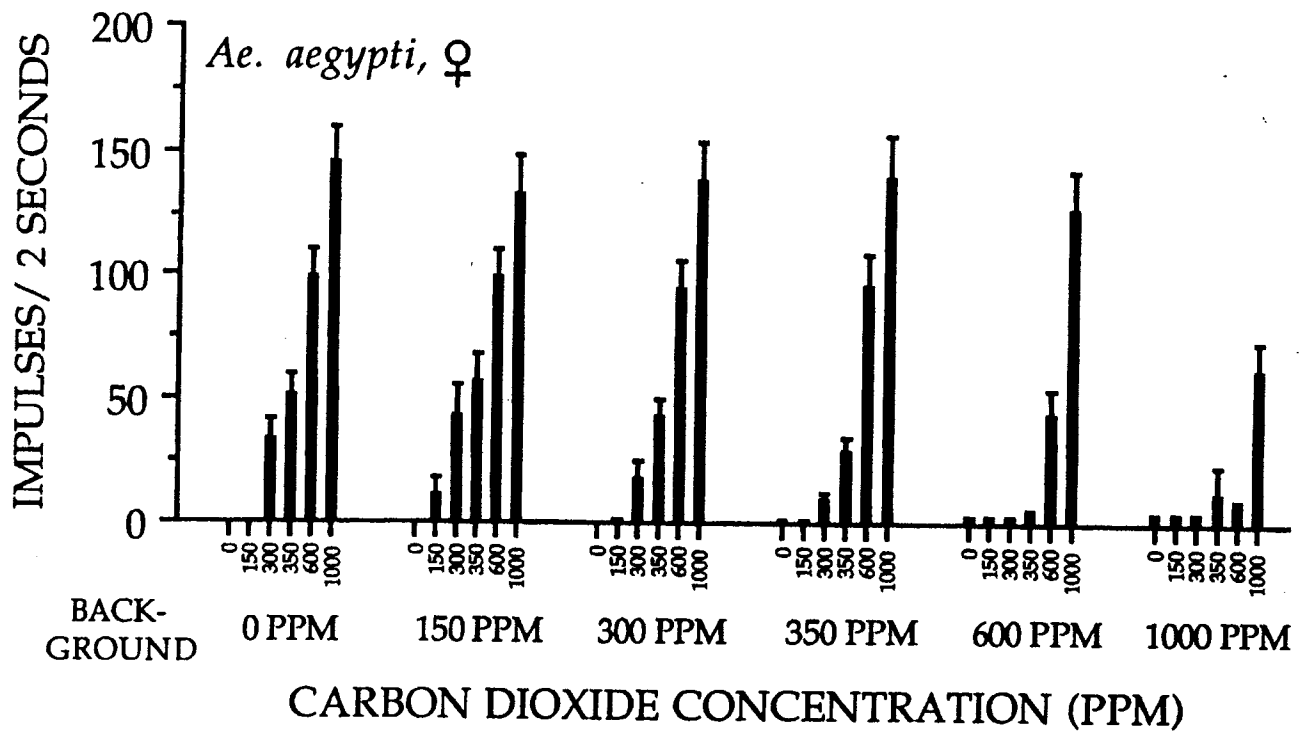


Fig. 4 Average responses (+ SEM) of CO₂ receptor neurons in 8 s. basiconica on the maxillary palps of 7 female *Ae. aegypti*. The stimuli were 2 s pulses of 6 different concentrations of CO₂ delivered from each of the indicated background levels of CO₂

Electrophysiological Responses of Receptor Neurons in Mosquito Maxillary Palp Sensilla to Carbon Dioxide

A.J. Grant, B.E. Wigton, J.G. Aghajanian, and R.J. O'Connell.
 Worcester Foundation for Biomedical Research, Shrewsbury, MA
 American Biophysics Corp., Jamestown, RI
 J. Comp. Physiol. A (1995) 177: 389-396

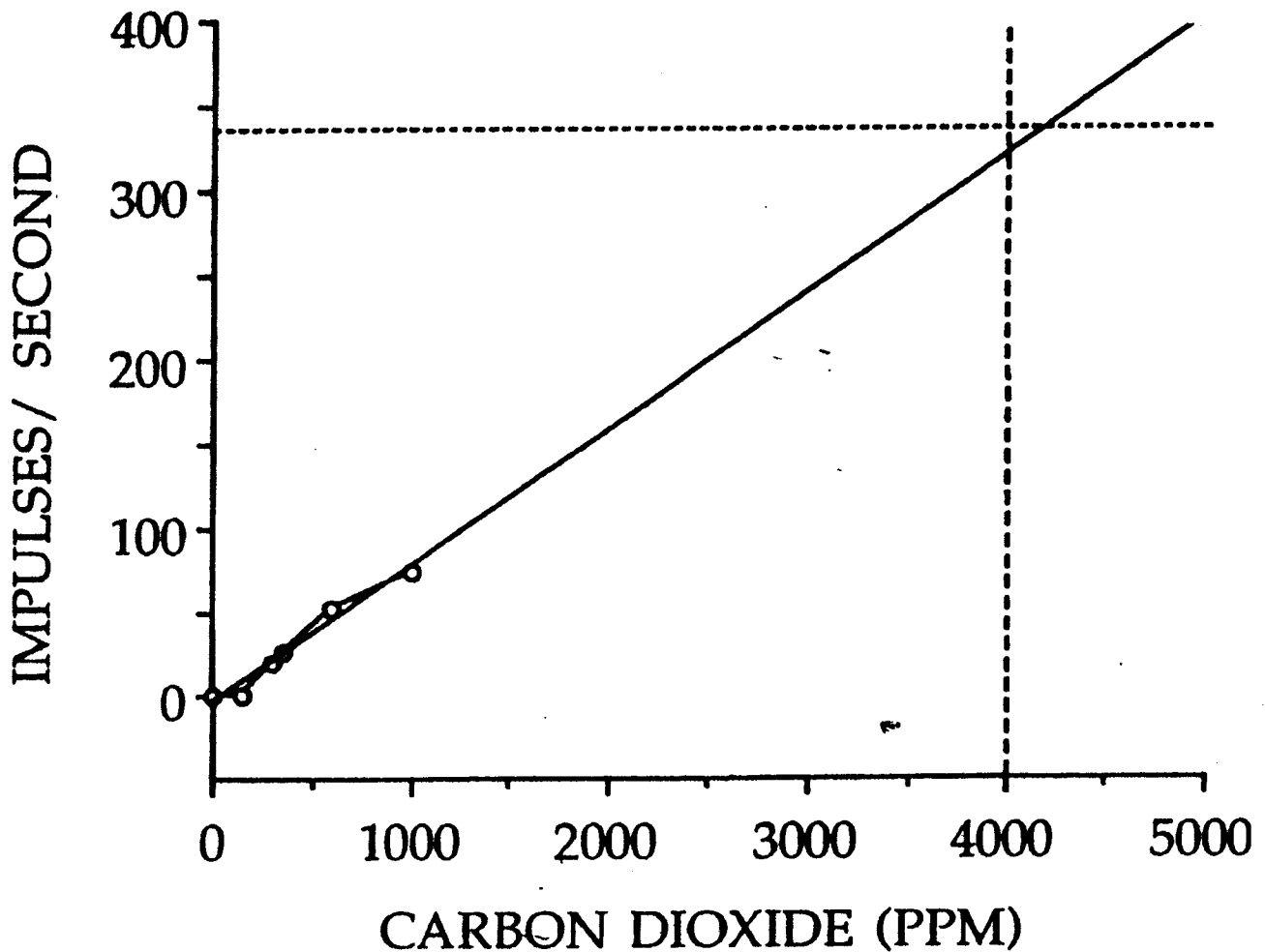


Fig. 6 The average response data from Fig. 2 is fitted to a straight line and the fitted line is extrapolated to a peak concentration of 4000 ppm CO₂, equivalent to the level reported in expired human breath

Electrophysiological Responses of Receptor Neurons in Mosquito Maxillary Palp Sensilla to Carbon Dioxide

A.J. Grant, B.E. Wigton, J.G. Aghajanian, and R.J. O'Connell.
 Worcester Foundation for Biomedical Research, Shrewsbury, MA
 American Biophysics Corp., Jamestown, RI
 J. Comp. Physiol. A (1995) 177: 389-396

Although Grant et al. did not measure the response at 4000 ppm, the argue for a linear response throughout a wide range of CO₂ concentrations.

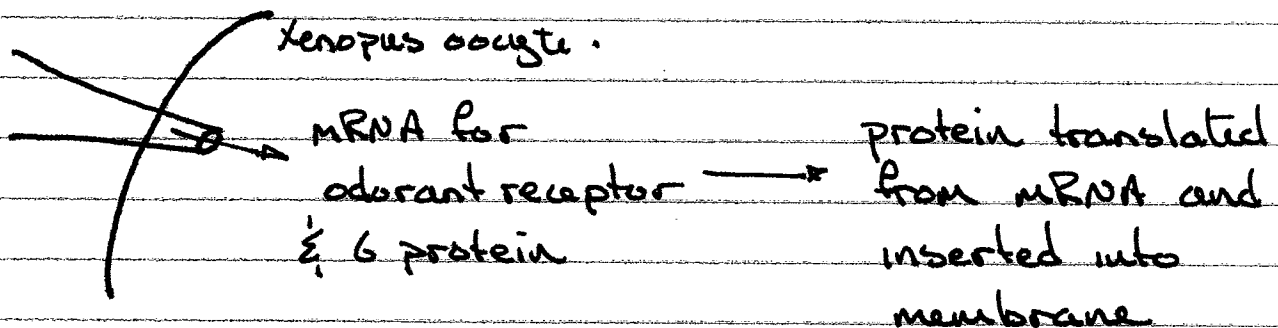
So, CO_2 receptors exist in mosquito (and other blood feeding) insects.

The sensitivity and dynamic range, unsaturated at 1000 ppm, imply the utility of CO_2 sensing as the bloodsucker seeks its prey.

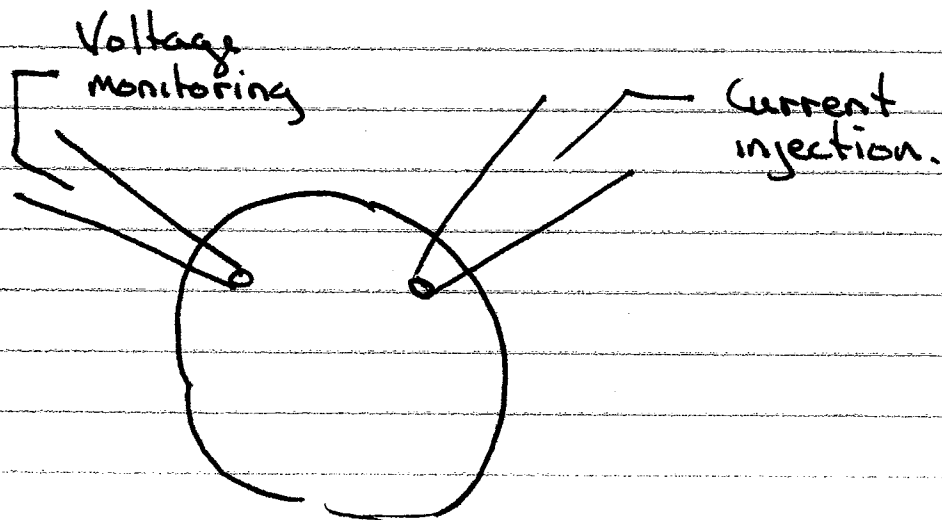
But, what are the underlying events that result in the generation of the action potentials measured extracellularly?

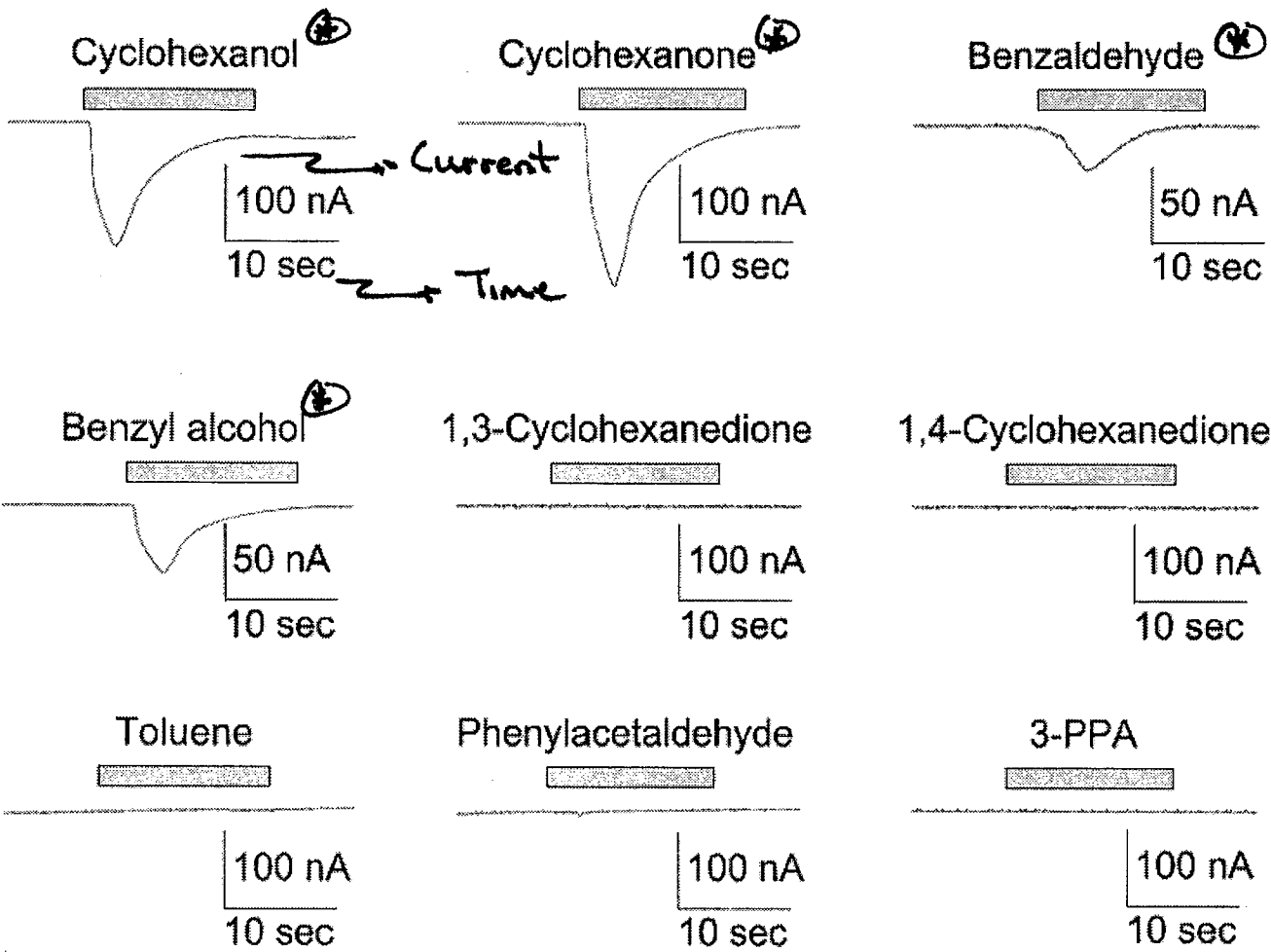
To explore this requires direct measurements, using intracellular techniques.

In one example (overhead/leaf):



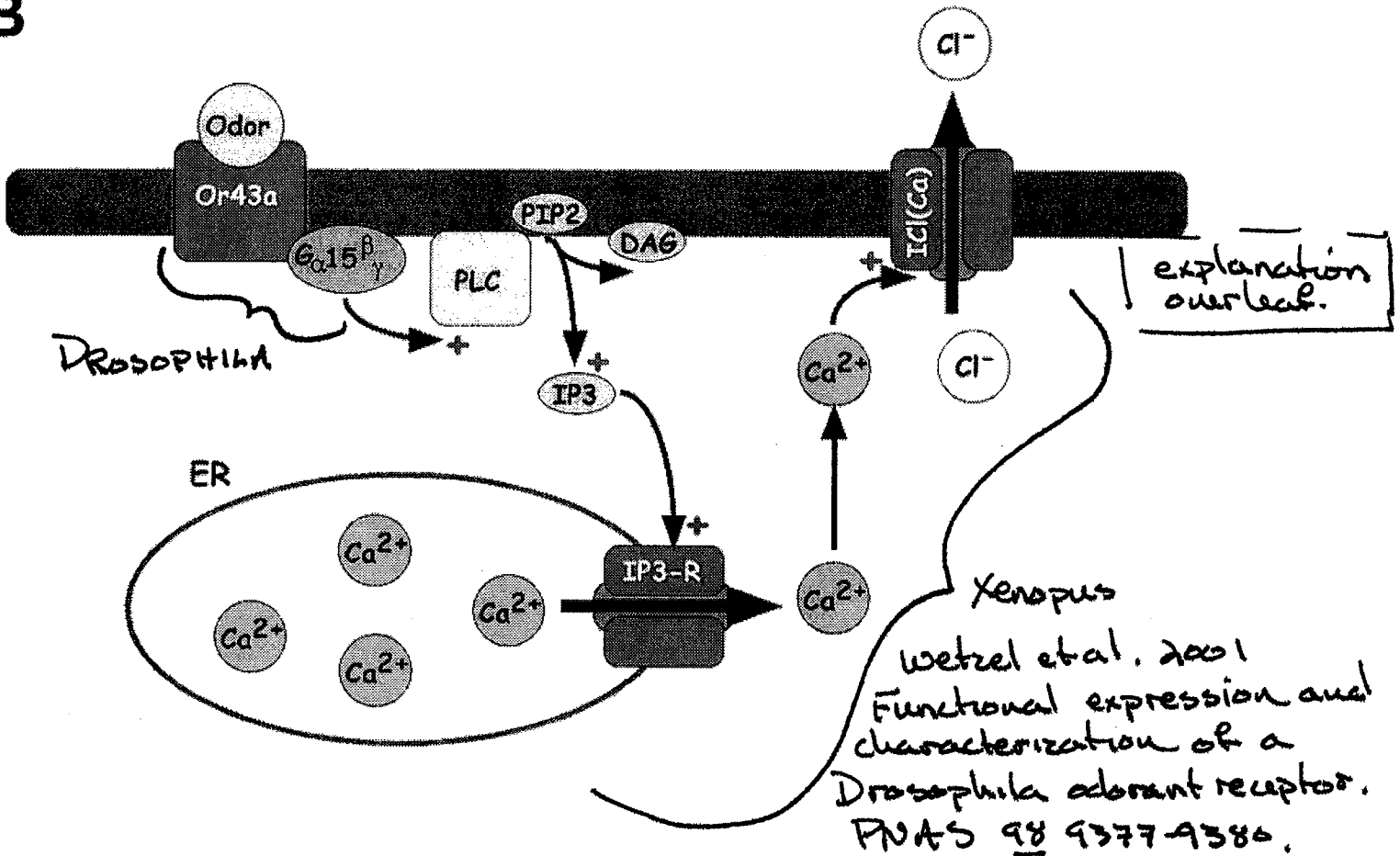
Now,





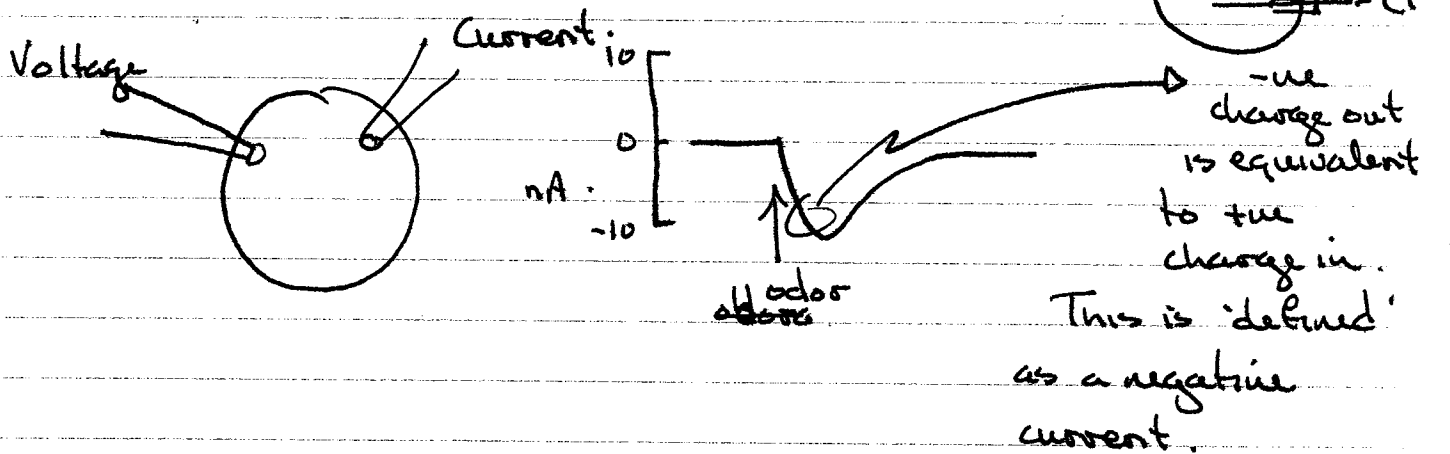
⊕ sensitive to these odors.

B



The patch technique is common for heterologous expression of transporters. The experiments are normally performed under Voltage Clamp.

Hold the voltage at a specified value, measure the current required to hold the voltage at that value.



But, what are the ion channels important in insects?

Very little work has been done, because the odor-receptor neurons are not accessible for intracellular measurements.

Instead, cultured neurons must be used. (e.g. Monica Stengl 1994 & Wegner et al. 1994).

M. Stengl: Insect olfactory transduction

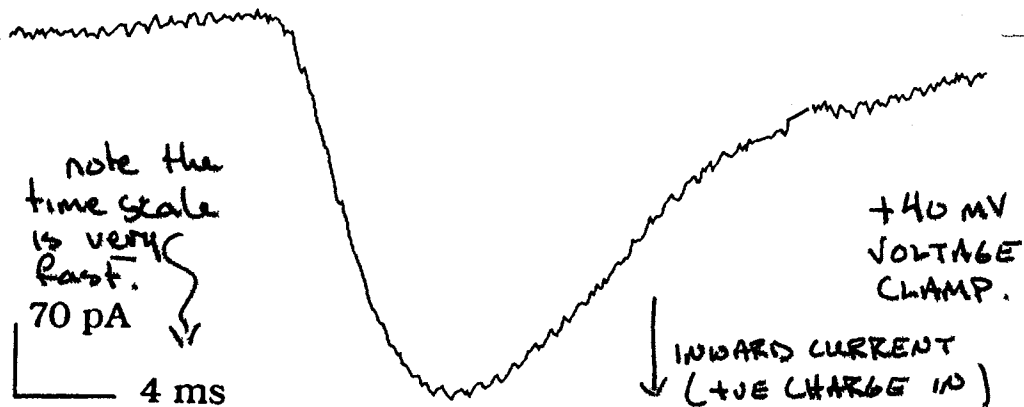
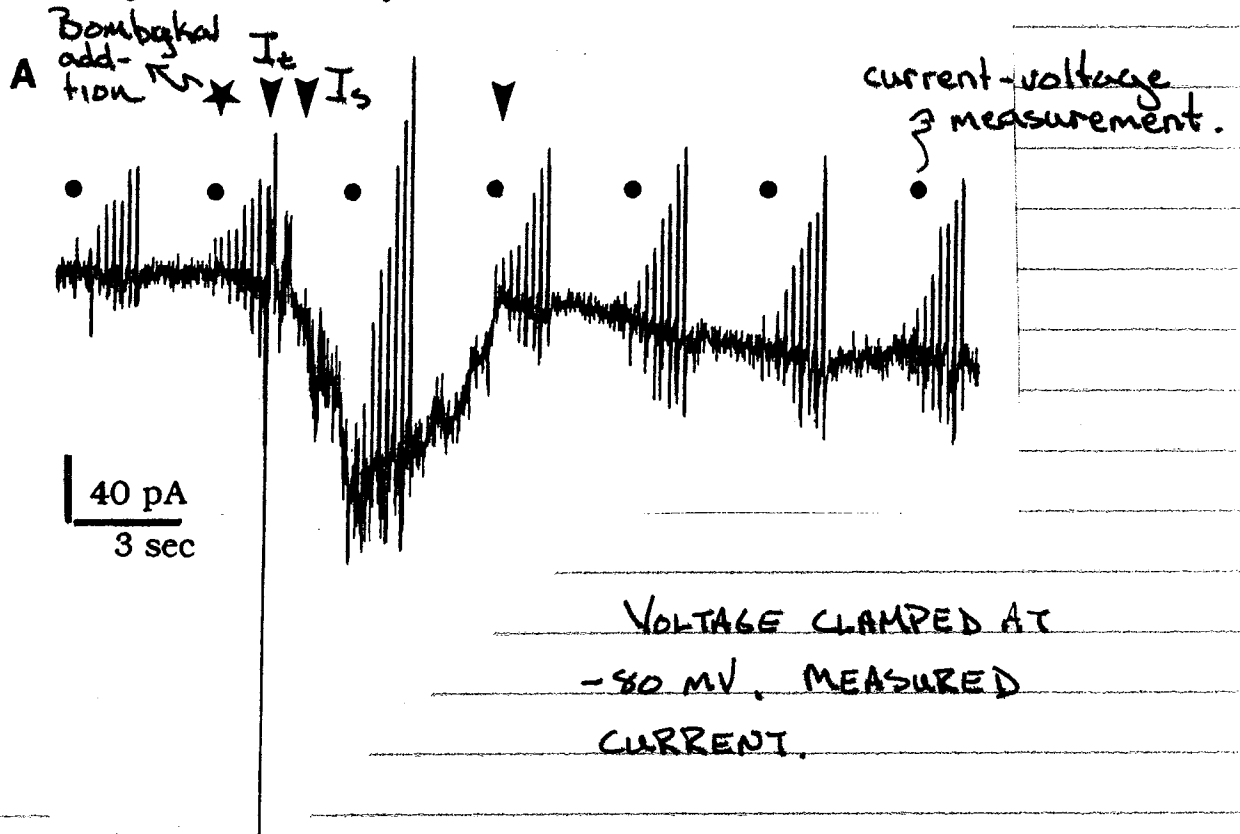
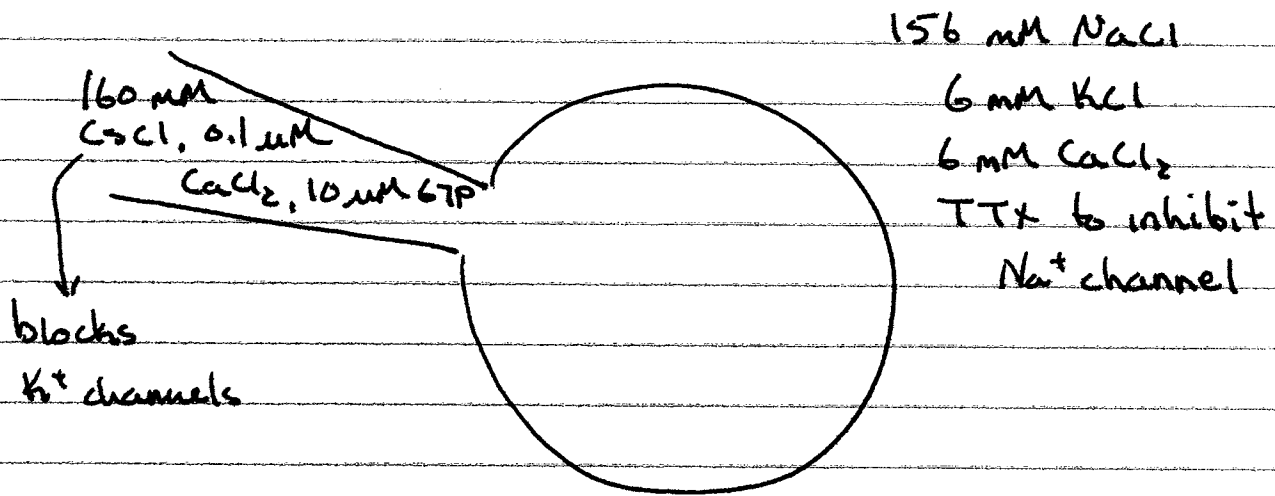


Fig. 2. The transient pheromone-dependent current I_t is not a cation current but a Ca^{2+} current, because it appears as inward current at 40 mV holding potential. Whole-cell current recording of 3 week cultured ORNs after application of 2 pg/ml bombykal in presence of Na^+ (0.1 μM TTX outside) and K^+ channel blockers (160 mM intracellular CsCl). Same recording as in Fig. 1A, current at first arrowhead at an expanded time scale. The zero current level is at the start of the record



$$E_{Ca} = \frac{55}{2} \cdot \log \frac{6}{0.0001} = +119 \text{ mV.}$$

Stengl observes inward current at both -80 mV & +40 mV, suggest the current is through an inward Ca²⁺ channel.

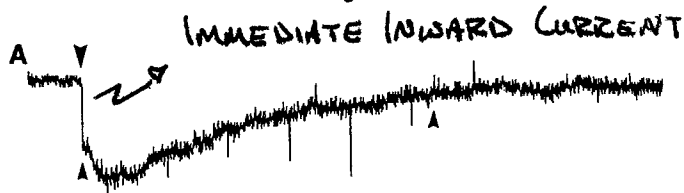
Additional evidence:

0 Ca²⁺ outside, no I_{Ca}

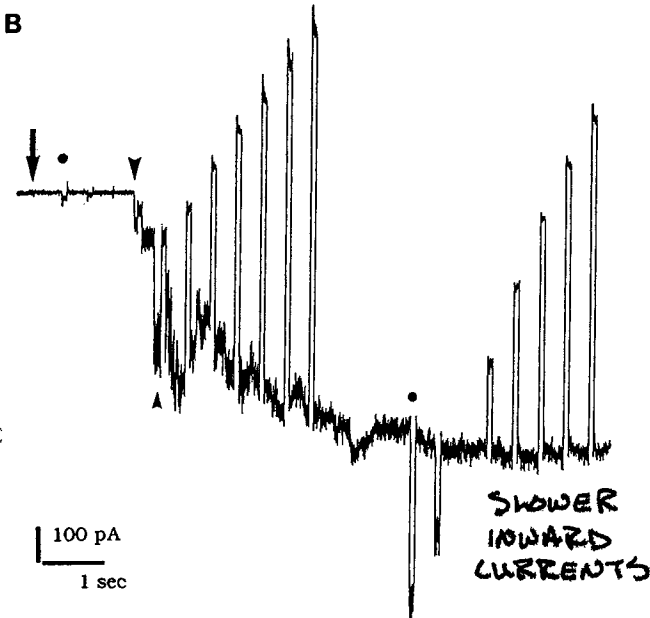
86 mM BaCl₂ outside, sustained I_{Ca}
(Ba²⁺ passes through Ca²⁺ channels)

Ni⁺ outside, no I_{Ca}
(Ni⁺ inhibits Ca²⁺ channels)

The slow I_s current has a reversal potential of ~0, thus it is a non-specific cation channel.

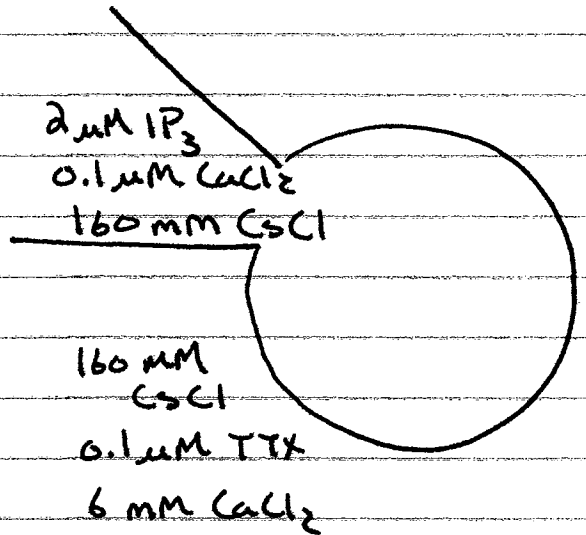


50 pA
1 sec



100 pA
1 sec

Fig. 4. Inositol-trisphosphate-dependent inward currents show at least 3 different elements at -80 mV holding potential in 6 mM external Ca^{2+} . Whole-cell voltage clamp recording at -80 mV holding potential of 3 week cultured ORN (with $2 \mu\text{M}$ IP_3 , 160 mM CsCl , $0.1 \mu\text{M}$ Ca^{2+} in the patch pipette and extracellular saline containing 160 mM CsCl , 6 mM Ca^{2+} and $0.1 \mu\text{M}$ TTX). A rapid inward current (*big arrowhead*) is superimposed on two more slowly developing inward currents (*1st and 2nd small arrowhead*). The beginning of the third inward current component cannot be distinguished in the record shown (it does not necessarily start at the *second arrowhead*). But the third inward current component becomes apparent when the 0 current level at the beginning of the record is compared to the stable inward current level at the end of the record. It is not known whether all inward transients have the same origin. **B** The second component of the IP_3 -dependent inward current is stable in $0.1 \mu\text{M}$ external Ca^{2+} . Same whole-cell recording of the same cell as in **A** after changing the extracellular saline to 160 mM CsCl , $0.1 \mu\text{M}$ Ca^{2+} , $0.1 \mu\text{M}$ TTX (*arrow*). Currents at -80 mV holding potential with superimposed currents elicited during voltage step protocols (*dots*, in 20 mV steps from -120 mV to 80 mV, to determine reversal potentials). The second element of the IP_3 -dependent currents (*small arrowhead*) is superimposed on the first inward current element (*big arrowhead*). The current traces are not shown in full length



external Ca^{2+}
changed to $0.1 \mu\text{M}$
 CaCl_2 .

VOLTAGE CLAMP at
 -80 mV.

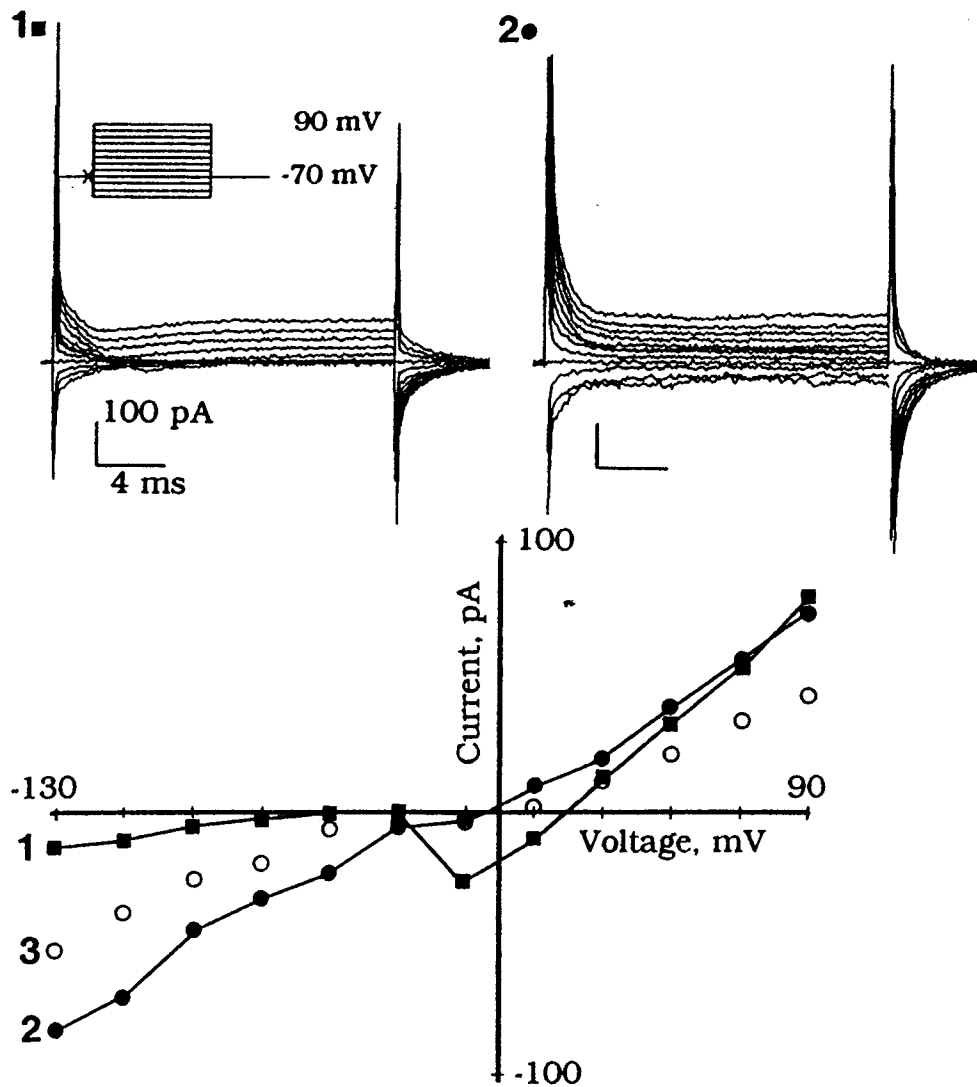


Fig. 5. The IP_3 -dependent cation current is preceded by a different IP_3 -dependent current with a positive reversal potential which occurs in the presence of Na^{2+} channel blockers. The current voltage plots of 3 consecutive recordings (numbered 1–3, separated by about 3 s) are shown with 156 mM NaCl, 6 mM KCl, 6 mM Ca^{2+} and 0.1 μM TTX outside, and with 100 μM IP_3 , 160 mM CsCl, 0.1 μM Ca^{2+} in the patch pipette. Only two of the respective current records with the voltage protocols applied are shown in the upper half. Voltage step protocols ranging from -130 mV to 90 mV in 20 mV steps were applied from a holding potential of -70 mV. The IP_3 -dependent inward current (*filled squares*) with a reversal potential around 20 mV is followed within less than 3 s by a cation current (*filled circles*). The cation current declines within less than 3 s in 6 mM external Ca^{2+} (*open circles*). The capacitive transients are not shown in full length

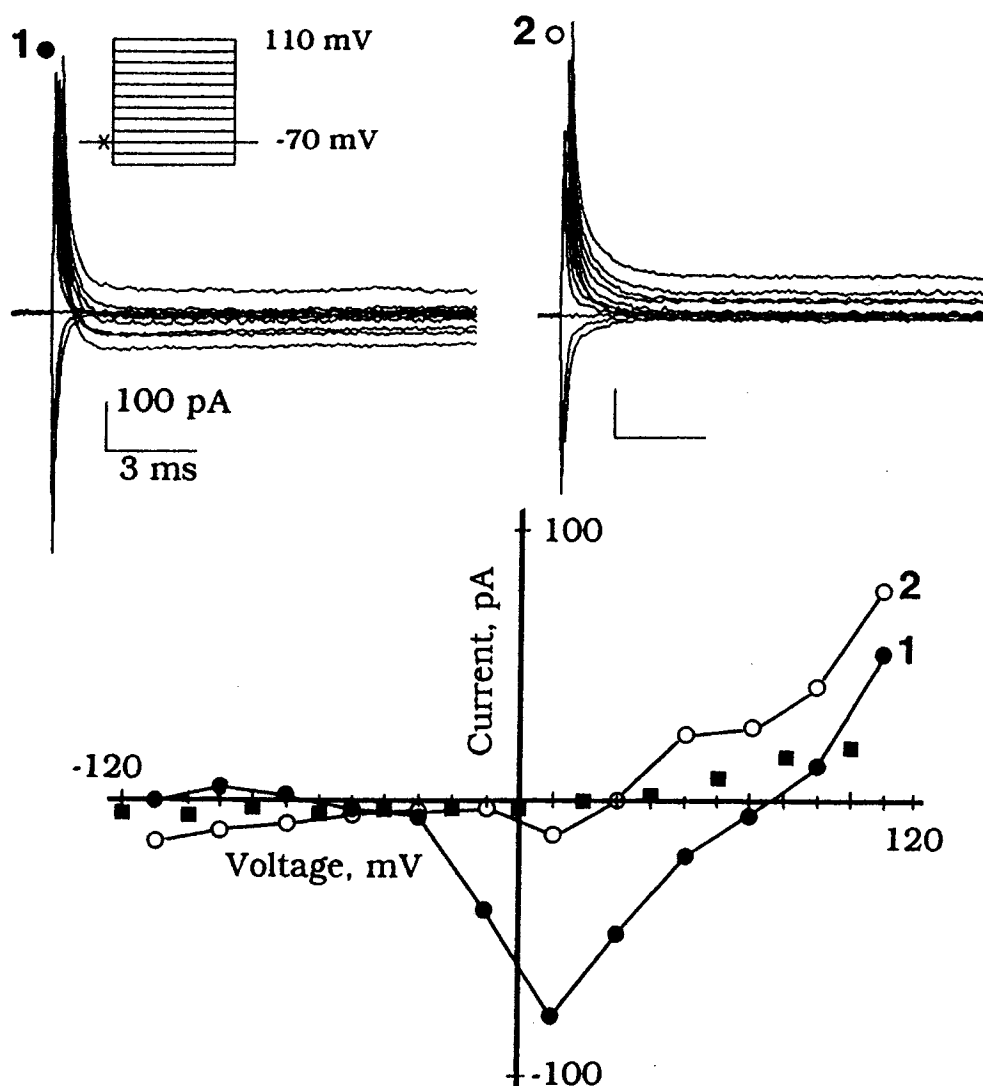


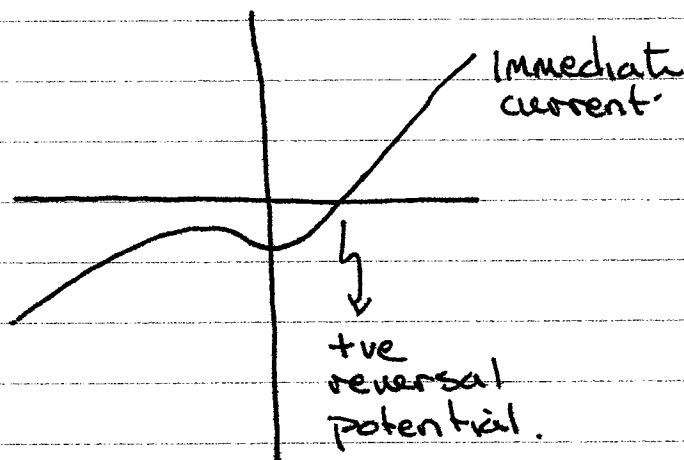
Fig. 6. The IP_3 -dependent Ca^{2+} current declines quickly in 6 mM external Ca^{2+} and does not occur in the presence of external Ni^{2+} . Whole-cell patch clamp recordings in extracellular saline containing 156 mM NaCl, 6 mM KCl, 20 mM TEA, 0.1 μM TTX with 6 mM Ca^{2+} outside and 100 μM IP_3 , 160 mM CsCl, 0.1 μM Ca^{2+} inside. Two consecutive current records from the same cell (1, 2, separated by 1 min 13 s) with the voltage step protocol applied is shown in the upper half. From a holding potential of -70 mV, voltage steps were applied from -110 mV to 110 mV. In the presence of the Ca^{2+} channel blocker 6 mM Ni^{2+} and 20 mM TEA no IP_3 -dependent inward currents with positive reversal potentials occur (full squares, different cell, recorded in 20 mV steps from -120 mV to 100 mV).

Biochemical assays of IP_3 showed that pheromone application caused IP_3 elevation within 50 msec, and decay within 100 msec: TRANSIENT ELEVATION.

Does IP_3 affect ion channel activity? Stenzel tests this by introducing IP_3 intracellularly in whole cell voltage clamp experiments.

In the presence of IP_3 , there was an immediate inward current, followed by slower inward currents.

The immediate inward current has the $I-V$ signature of an IP_3 -activated Ca^{2+} channel.



which is inhibited by Mg^{2+}

SECOND MESSENGER-CONTROLLED MEMBRANE CONDUCTANCE

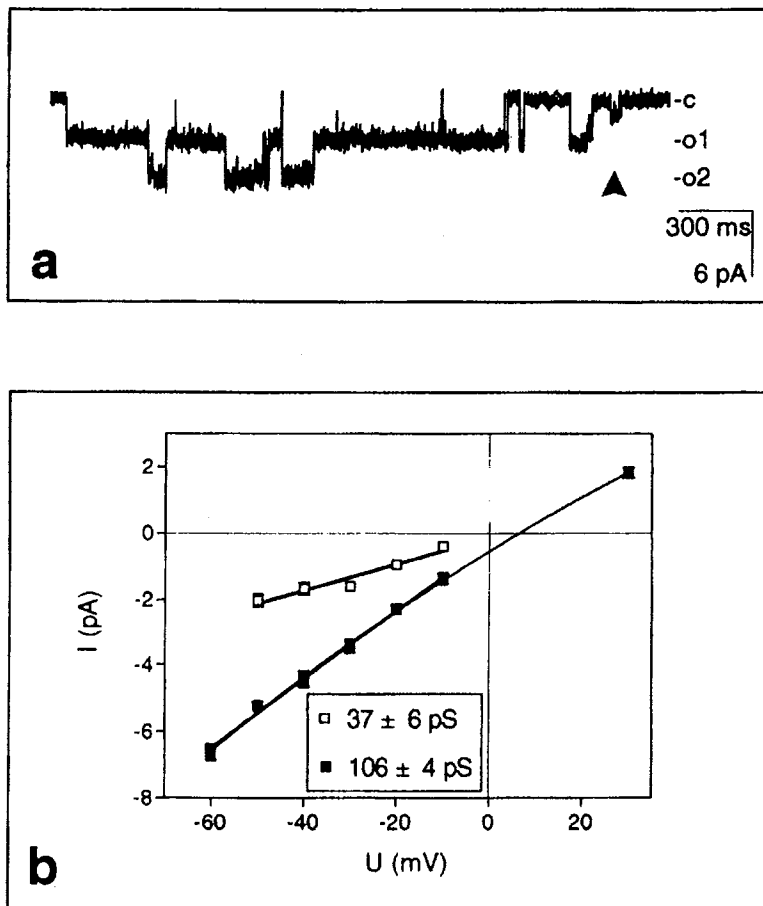
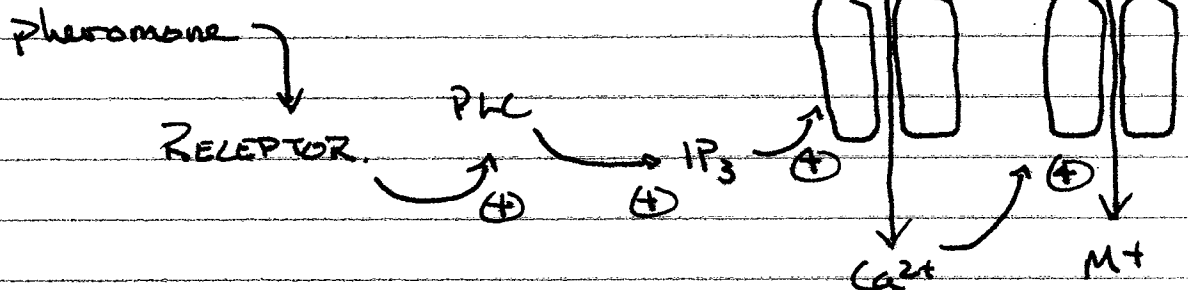


FIGURE 4. Ion channel activity in the presence of intracellular IP_3 . (a) Inward-directed channel fluctuations of two types of ion channels were observed in the outside-out configuration of the patch-clamp technique. The trace shows the activity of two channels displaying the identical current amplitudes and of one channel exhibiting a small current amplitude (arrow). The trace was recorded at a holding potential of -30 mV. Single channel states were indicated to be the closed (c) or the open state (o). IP_3 was present in the pipette solution at a concentration of $100 \mu M$. (b) A current-voltage relationship is demonstrated for the channel types shown in (a). Their conductances were calculated to be 106 ± 4 and 37 ± 6 pS. The pipette solution contained (in mM): CsCl 130, NaCl 10, LiCl 10, KCl 2, EGTA 1, $CaCl_2$ 0.6; Tris/Cl 10, IP_3 0.1; pH 7.4 was adjusted with HCl. The composition of the bath solution was (in mM): $BaCl_2$ 50, NaCl 10, choline-Cl 10, Tris/Cl 10; pH 7.4 was adjusted with HCl.

Wegener et al. 1997 J. Insect Physiol. 43 595-605

MODEL.



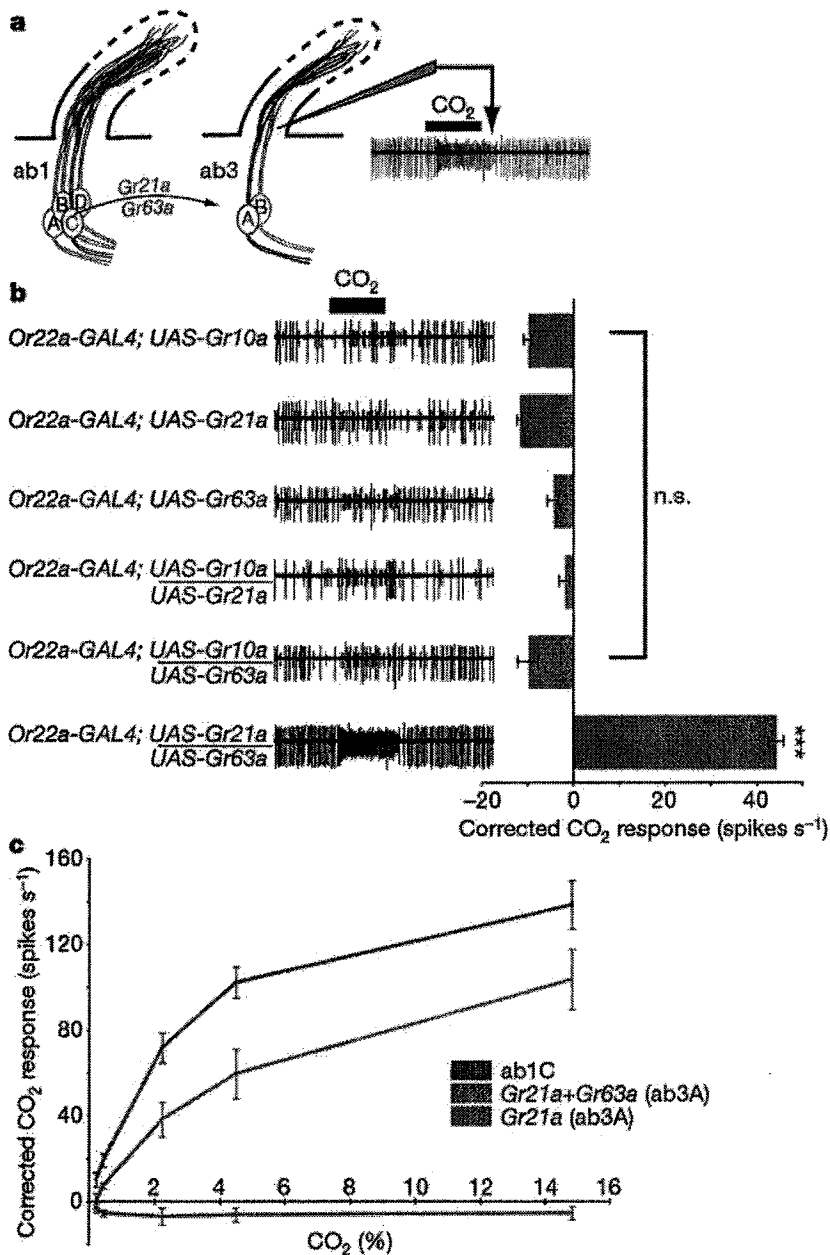
Note that Na^+ & K^+ channels were inhibited by TTX & (Ca^{2+} & TEA) so that an action potential would not occur (obscuring the initial electrical changes).

There is direct evidence for an IP_3 -activated channel on the plasma membrane:
in locust[Ⓢ]:

In outside-out patches, two ion channels ($G = 37 \text{ pS}$ & $G = 106 \text{ pS}$) were observed that were, at least, Ca^{2+} permeable.

Ⓢ Wegner, J.W., W. Hanke, H. Breer 1997 Second messenger-controlled membrane conductance in locust (*Locusta migratoria*) olfactory neurons. *J. Insect Physiol.* 43 595-605.

Expression of both Gr21a and Gr63a confers CO₂ sensitivity on normally CO₂-insensitive neurons.



a, Diagram outlining the methodology for the transfer of the CO₂ receptor to the ab3A neuron. Extracellular recording of spikes emitted by CO₂ is at the right. **b**, The indicated combinations of antennal gustatory receptor genes were ectopically expressed in ab3A neurons using the Or22a-GAL4 driver. Single-sensillum electrophysiological recordings on transgenic ab3 sensilla, recognized by their characteristic response to ethyl hexanoate (ab3A) and 2-heptanone (ab3B)17, were made for both room air (ca 0.035% CO₂) and ca 3% CO₂. Representative traces (stimulus bar, 1 s) are on the left, and mean responses (± s.e.m.) are on the right (n = 15–18 sensilla per genotype). Significant responses to CO₂ are only found with the combination of

Gr21a and Gr63a (Tukey HSD test; $P < 10^{-6}$). n.s., not significant. **c**, Dose–response curves for the combination of Gr21a and Gr63a (blue curve) versus expression of Gr21a alone (green curve) in ab3A neurons as compared to the CO₂ response in native ab1C neurons (red curve). Mean responses (s.e.m.) are plotted (n = 10 sensilla per genotype).

Jones WD, P Cayirlioglu, IG Kadow and LB Vosshall (2007) Two chemosensory receptors together mediate carbon dioxide detection in *Drosophila*. *Nature* 445:86–90.